

2D Materials for Spintronics and Quantum Sensing

WRT-1046

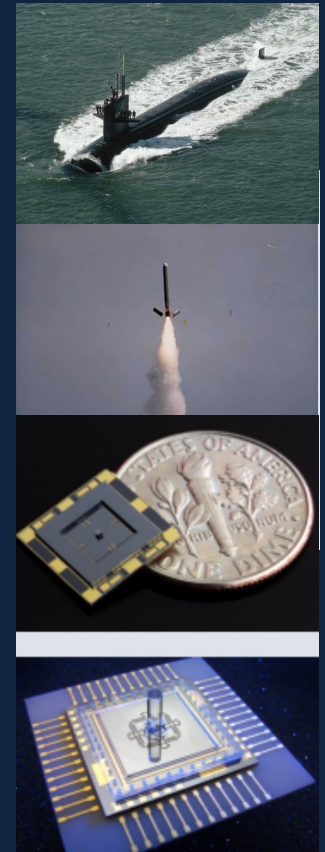
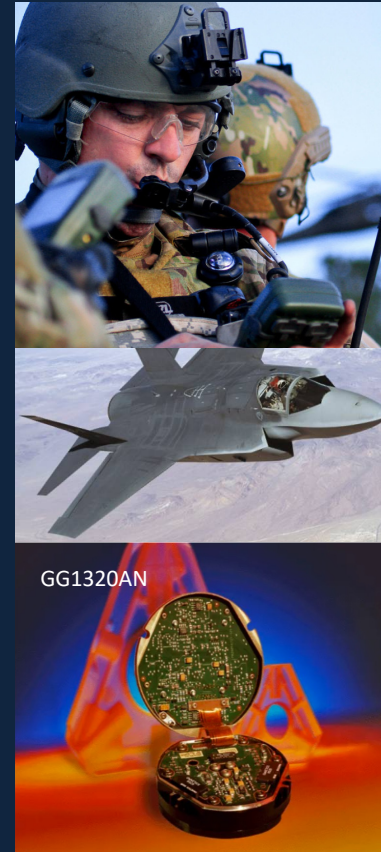
PI: EH Yang

Collaborators: C. Qu, S. Strauf (Stevens), A. Cummings (Catalan Inst. Nanoscience and Nanotech.), and G. Hader (CCDC-AC)

STEVENS
INSTITUTE OF TECHNOLOGY

Gyroscopes – Needs and Challenges

- The need for *alternatives to GPS* is evident as the GPS signal sees real threats due to local jammers denying access in the region.
- *Optical gyroscopes* are widely used for inertial navigation, stabilization and positioning control systems. However, the substantial increase in cSWaP is not conducive to the existing volume constraints.
- *MEMS gyroscopes* - vendors' specifications are listed only after standard testing, and do not include the shift-after-shock bias, scale factor or misalignment after the shock event.



Sagnac Interferometers

- 1913, Sagnac proposed the idea of using a ring interferometer as a rotation rate sensor in order to detect “the effect of the relative motion of the ether.”

Optical gyroscopes

- no moving parts
- 0.01 degree/hr bias stability
- HRG costs > \$1M
- 50 cm³, 19 lb, 30W

Atom Gyroscopes

- sensitivity ($Mc^2 / \hbar\omega \sim 10^{10}$): 60 μ degree/hr bias stability
- operation at ~ 100 nK, high vacuum, high magnetic fields
- Very heavy: several hundred kilograms

Electron interferometers:

- $Mc^2 / \hbar\omega \sim 10^6$
- Solid-state device: low fabrication costs, light weight, and direct integration with solid state electrical circuits

Surprisingly no discussion on gyroscopes; only experiments were done with electron beams in vacuum.



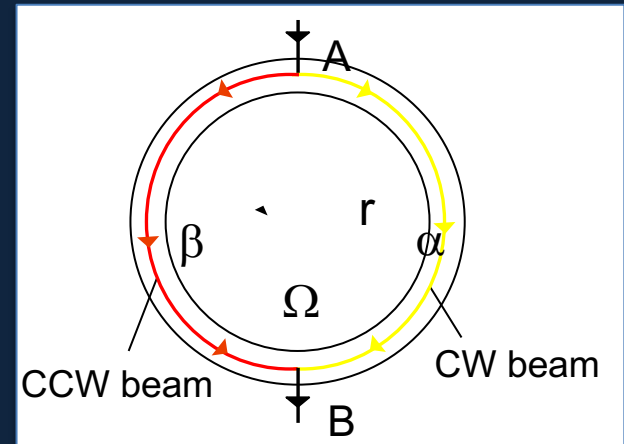
Atom gyroscopes

Matter Wave Interferometers

- 1913, Sagnac proposed the idea of using a ring interferometer as a rotation rate sensor in order to detect “the effect of the relative motion of the ether.”
- In 1924 de Broglie proposed that ordinary “particles” such as **electrons**, protons, or bowling balls could also exhibit wave characteristics in certain circumstances.
- For de Broglie matter waves, the phase difference is where is the enclosed area of the interferometer, the rotation rate, the particle mass, and is Planck’s constant.

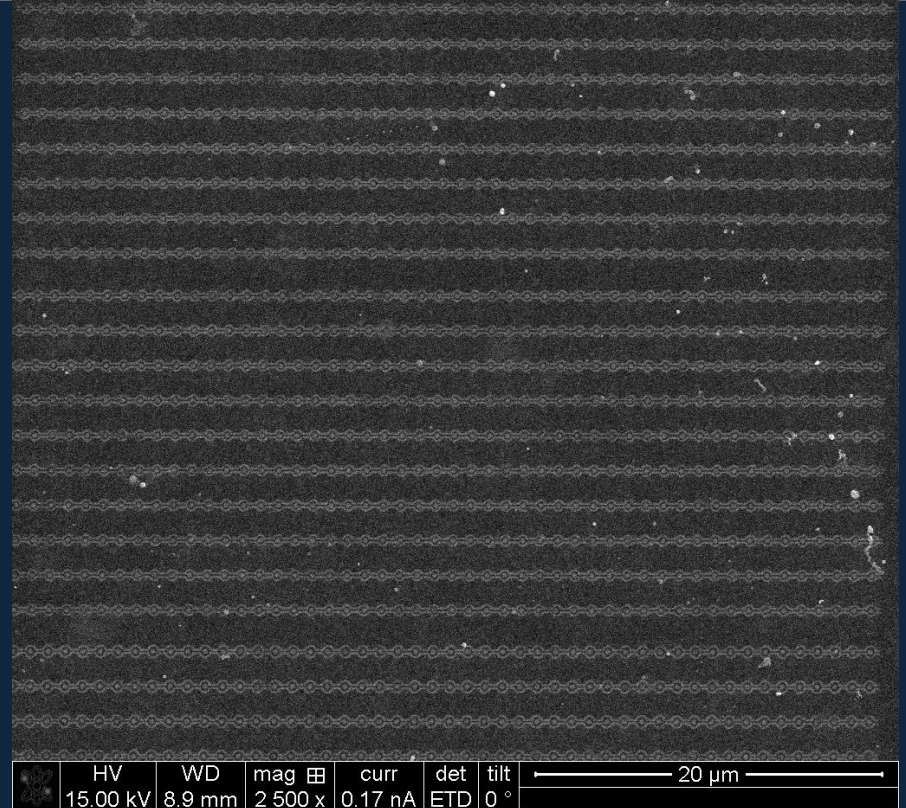
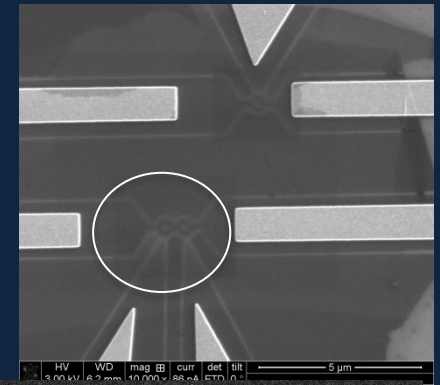
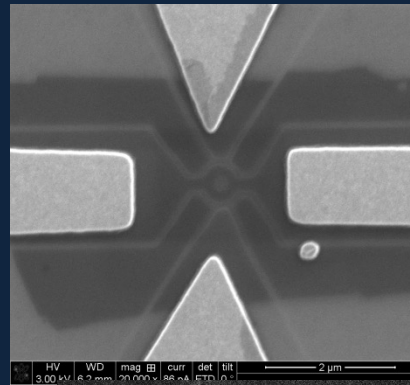
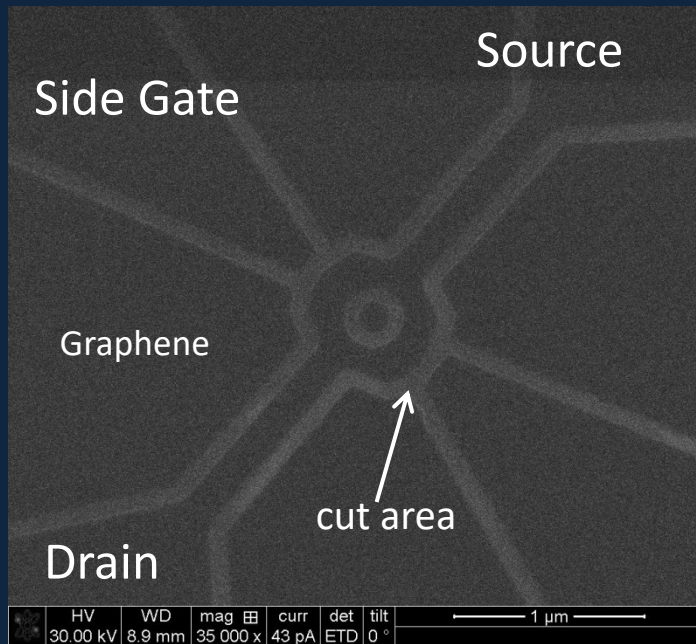
$$\delta\varphi_{\alpha\beta} = \frac{2Am}{\hbar} \Omega \text{ for matter waves}$$

The measured signal would be larger than an optical interferometer, which is the ratio of the energy of massive particle to that of a photon.



Graphene Patterning toward Solid-State Interferometers

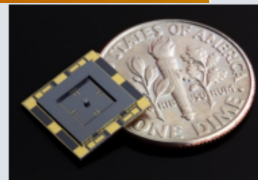
Single Ring Device



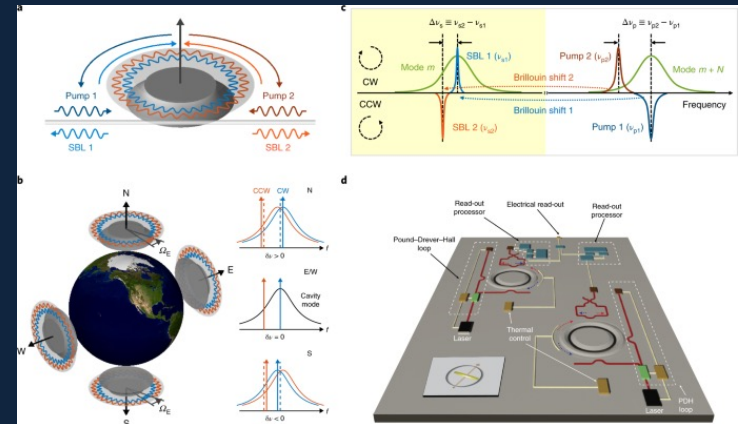
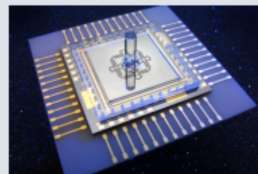
How to test Sagnac effect in graphene ring structures under development?



(Tang, 1998) All silicon, closed loop cloverleaf micro gyro (1.0 deg/hr)



(Wiberg, 2002) Meso-scale, post resonator gyro (0.1 deg/hr)



Nat. Photonics **14**, 345–349 (2020)



Aharonov-Bohm (AB) Interferometer

- Aharonov-Bohm effect: the oscillations in the resistance of a conducting ring as a function of an external magnetic flux piercing the ring.
- The Aharonov-Bohm phase shift φ_{AB} , is

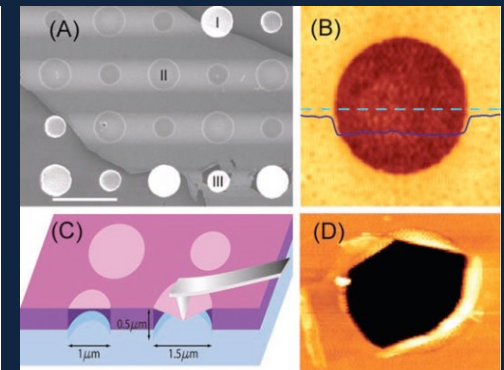
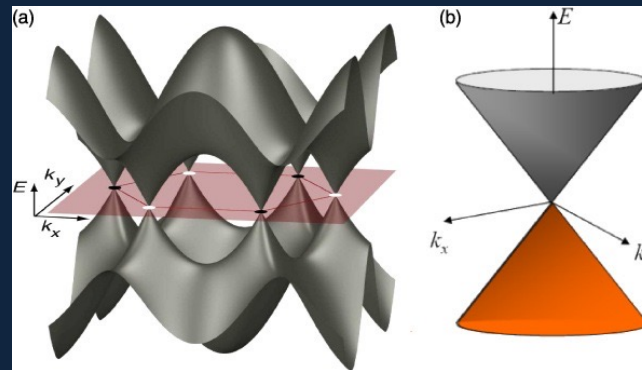
- $$G = G_Q \frac{(1 - \cos \chi)(1 + \cos^2 \varphi_{AB})}{\sin^2 \chi + [\cos \chi - (\cos \varphi_{AB})/2]^2}$$

where G_Q is the conductance quantum, χ is the electron phase shift when traveling between scatters, and φ_{AB} is the gauge-invariant combination of the phases.

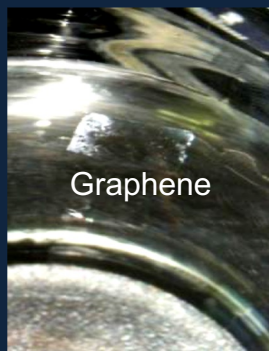
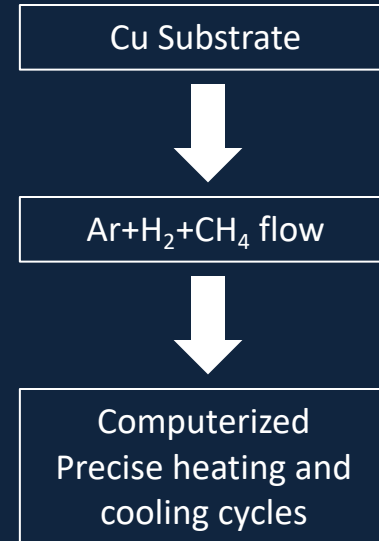
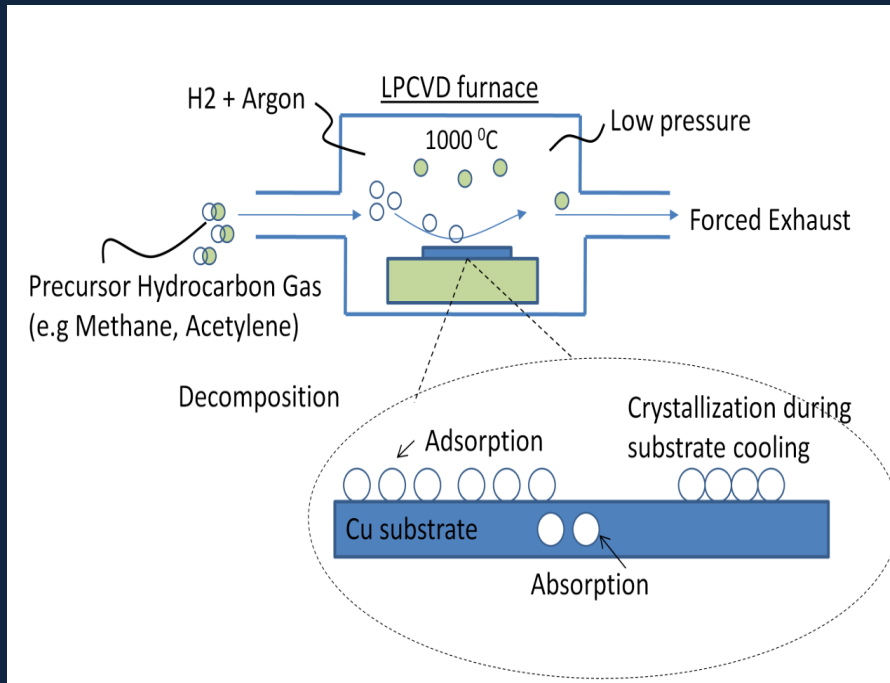
- Magnetoconductance measurements show fringes as a function of the applied magnetic field, characterized by fringe contrast and used to sense magnetic fields.
- An interferometer based on AB oscillations is in principle equivalent to a rotation sensor.

What materials we should use for solid-state electron interferometers?

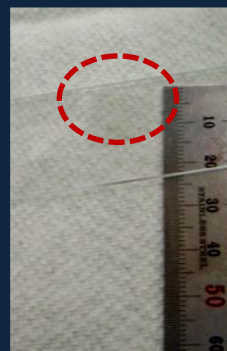
- Although scientists knew graphene existed, no-one had worked out how to extract it from graphite, until it was isolated in 2004 by Geim and Novoselov who received Nobel Prize (2010).
- Graphene has become a valuable nanomaterial due to its exceptionally high tensile strength, electrical conductivity, and transparency.
- Graphene acts as a 2D ballistic, phase coherent electron system with long phase coherence length that exceeds **5 μm** . (Science, 317(5844), 1530 (2007))



CVD Graphene Growth



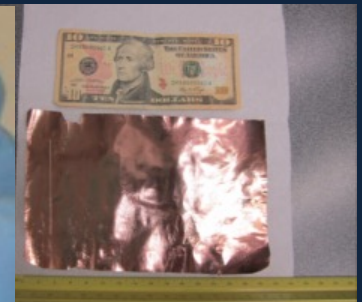
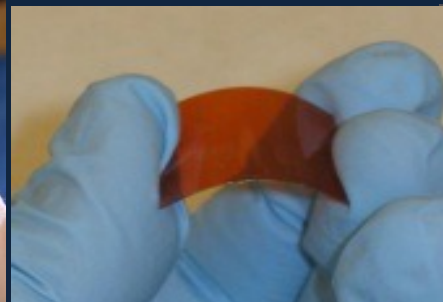
Graphene on water



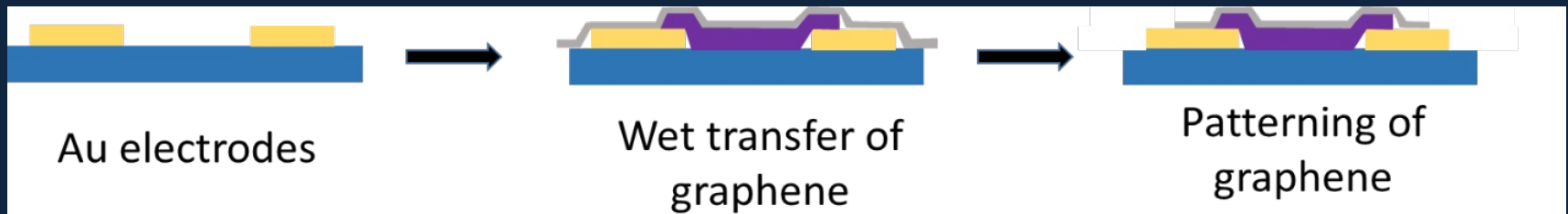
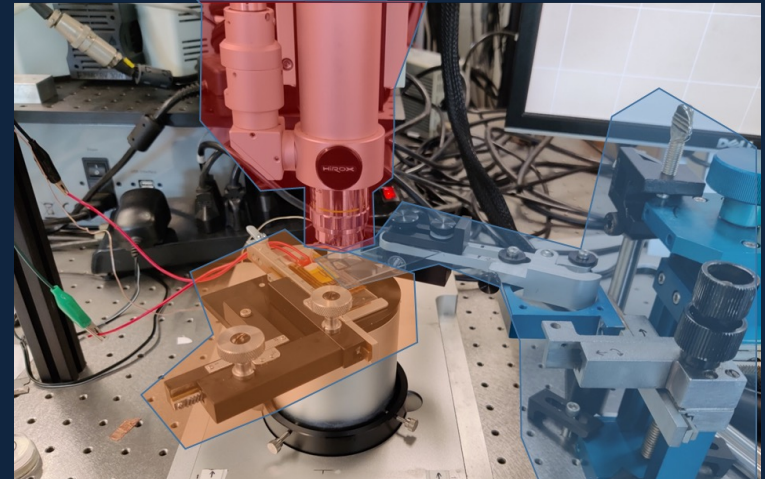
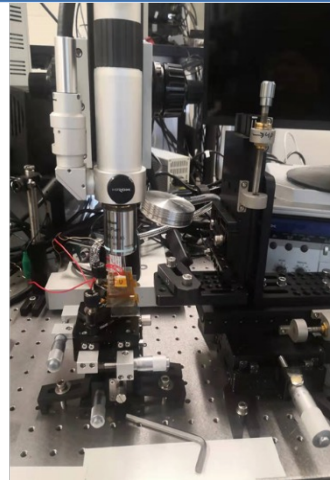
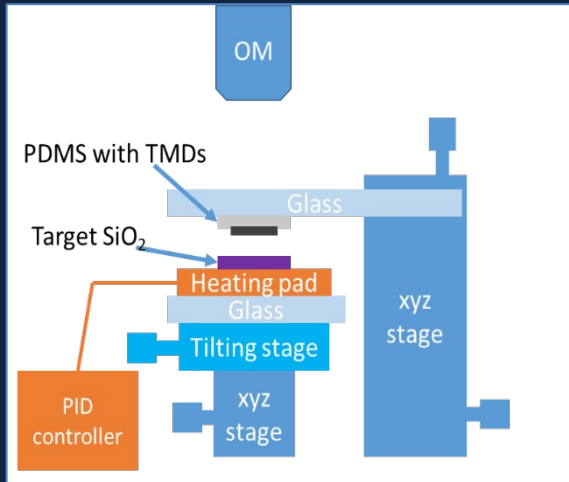
Transferred graphene on glass



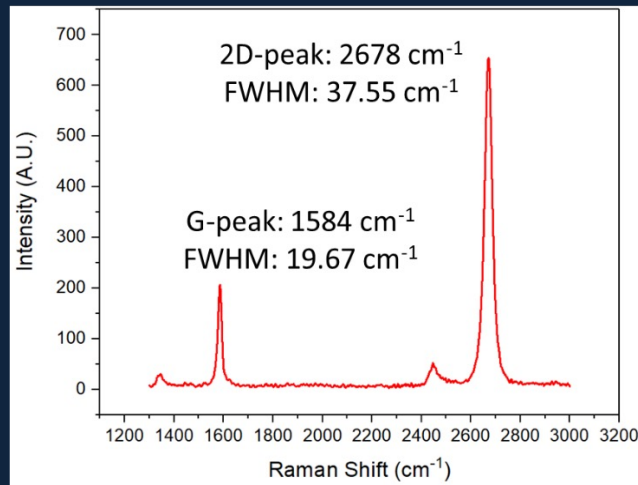
Transferred graphene on flexible substrate



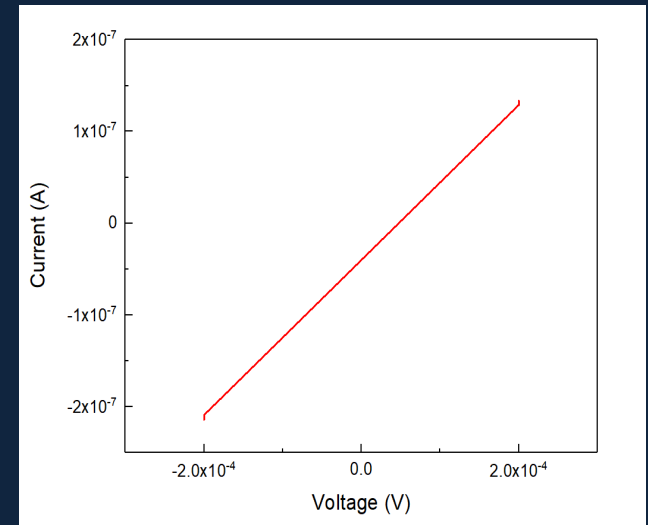
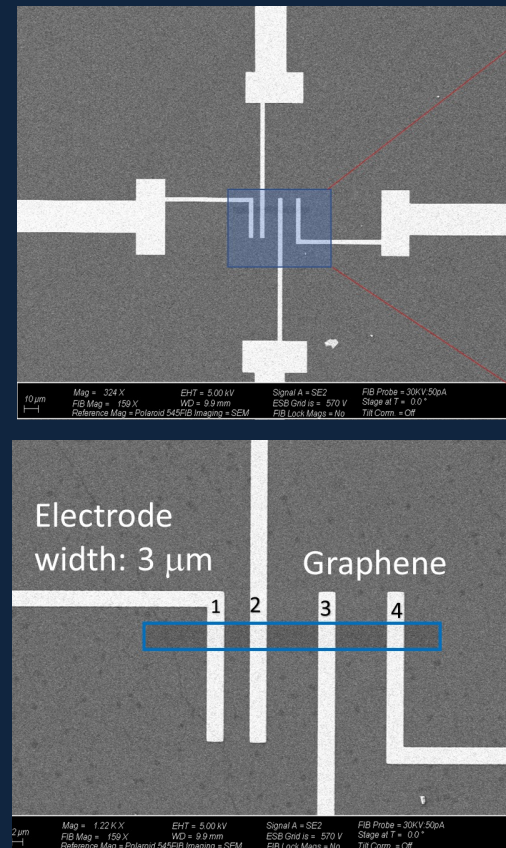
Graphene Device Fabrication



Characterization of Material Qualities

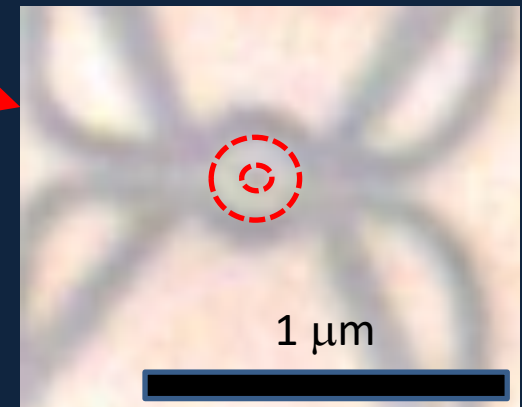
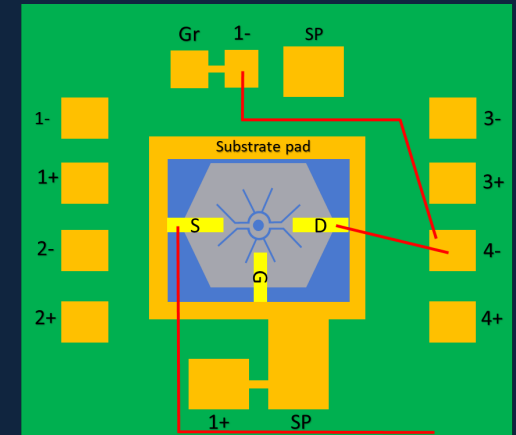
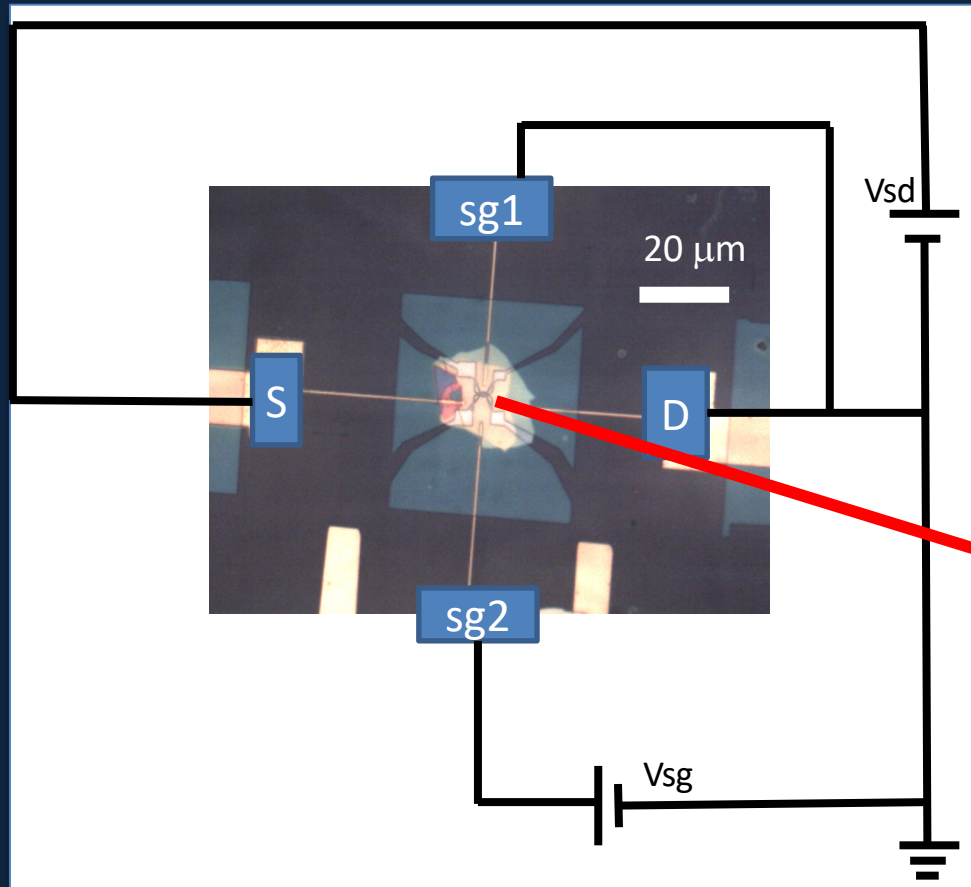


Raman spectra from a graphene ring

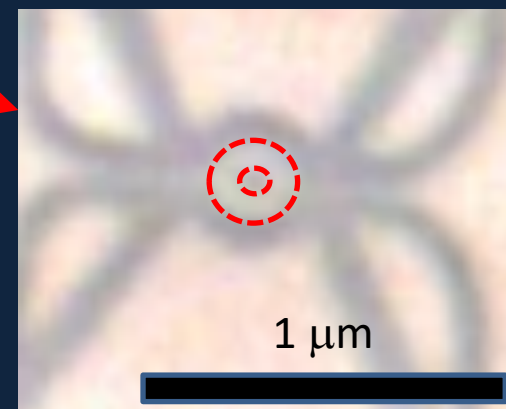
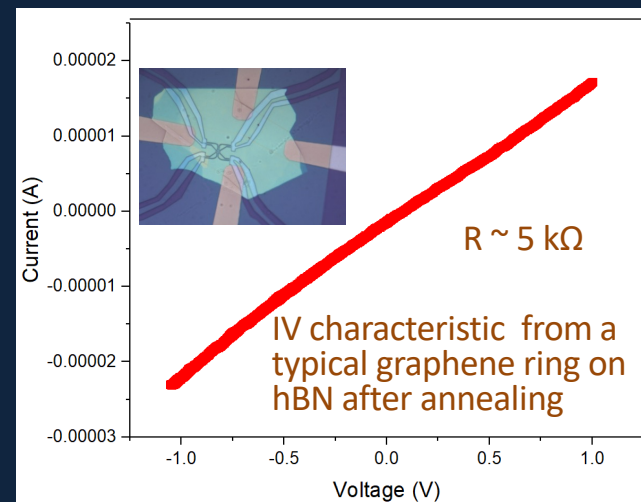
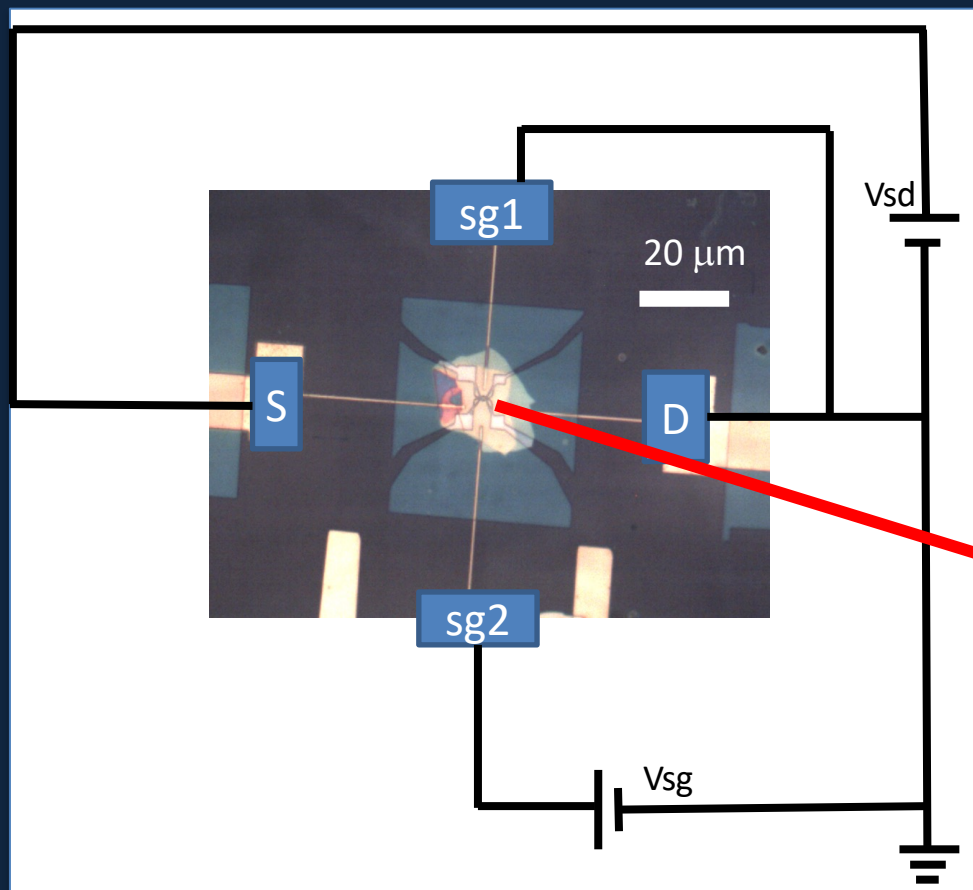


IV curve from channel 1-2
Channel Length: $4.74 \mu\text{m}$
Resistance: $\sim 1 \text{ k}\Omega$

Graphene Ring Fabrication



Graphene Ring Fabrication



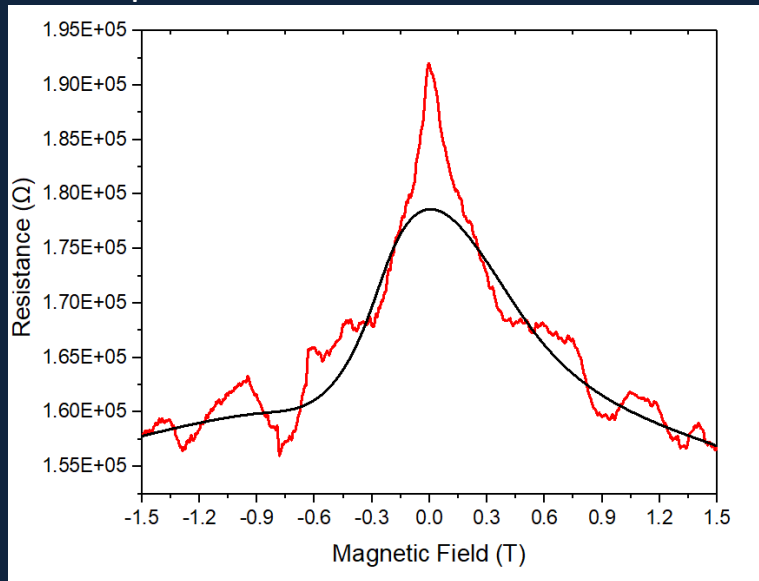
Conductance Oscillations under Magnetic Fields

Magnetic fields: -1.5 to 1.5 T.

Source-Drain voltage (V_{sd}): 4 mV.

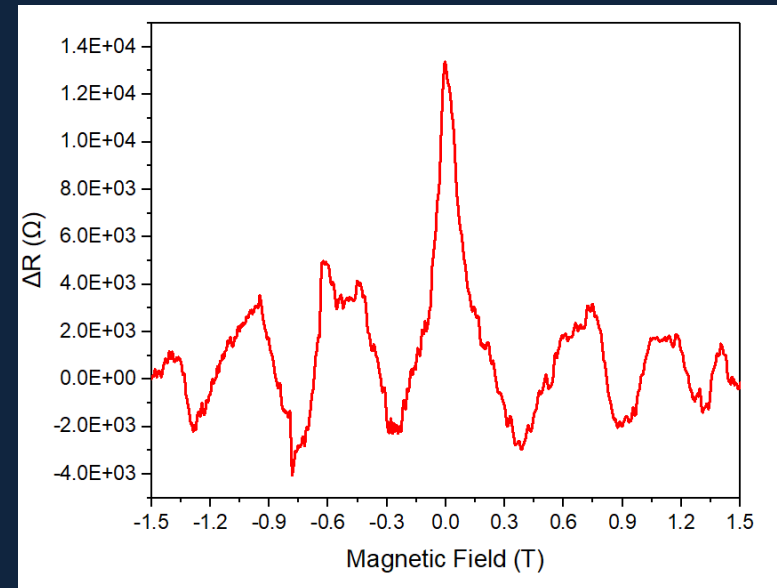
Side gate voltage (V_{sg}): 99 mV

Temperature: 4 K



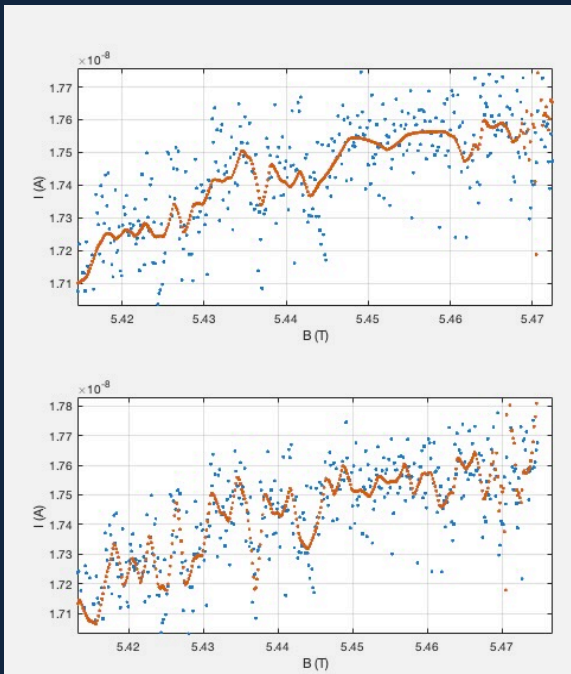
Low frequency background resistance (black) & magnetoresistance (red)

Landau level quantization effect

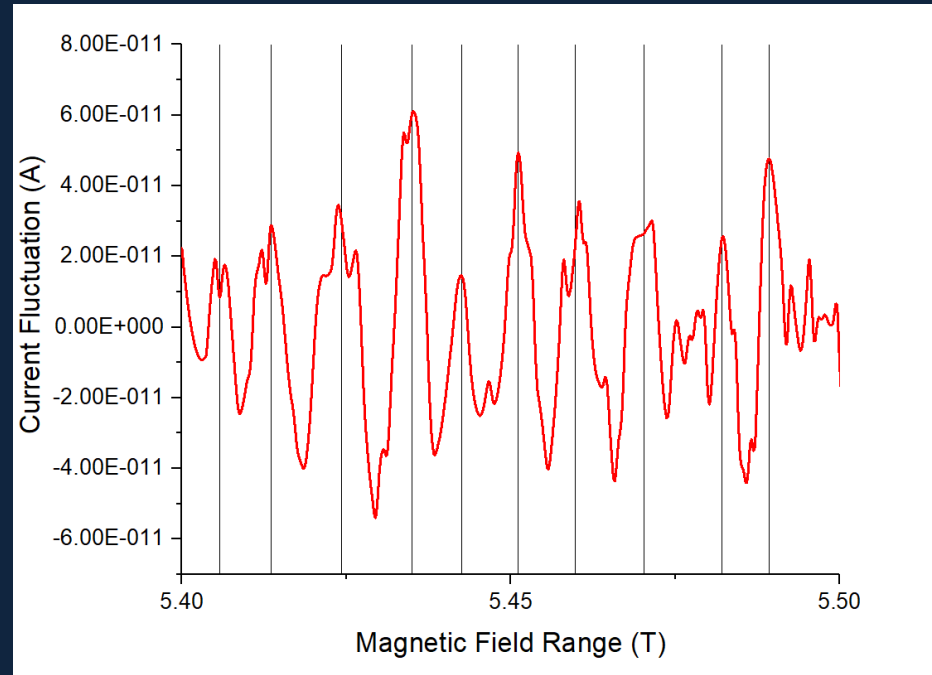


Oscillations obtained after baseline subtraction

Baseline Subtraction

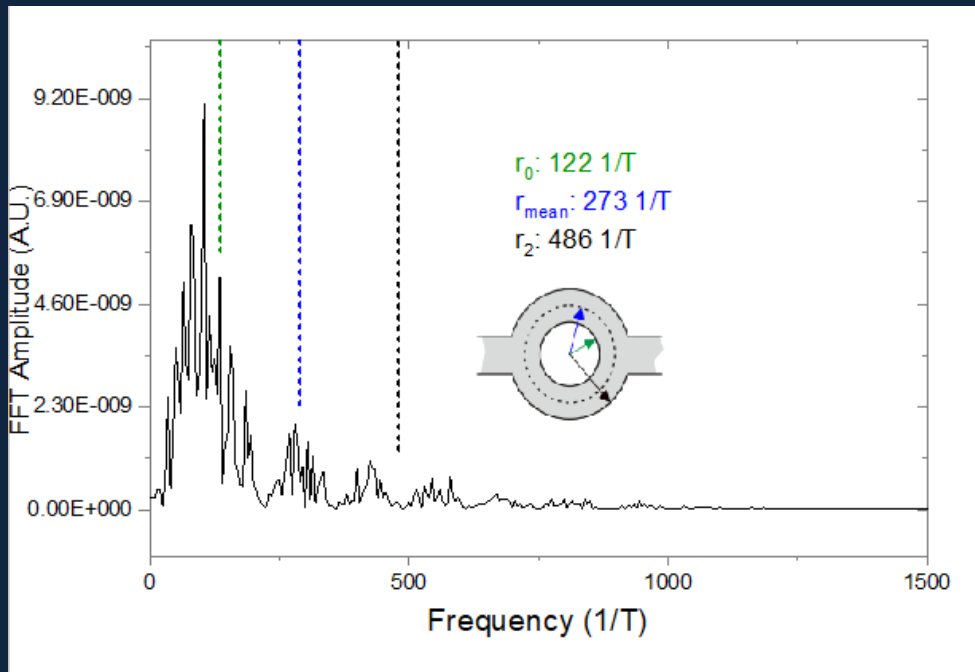


Levels denoising (red curves)
and magnetoresistance data.

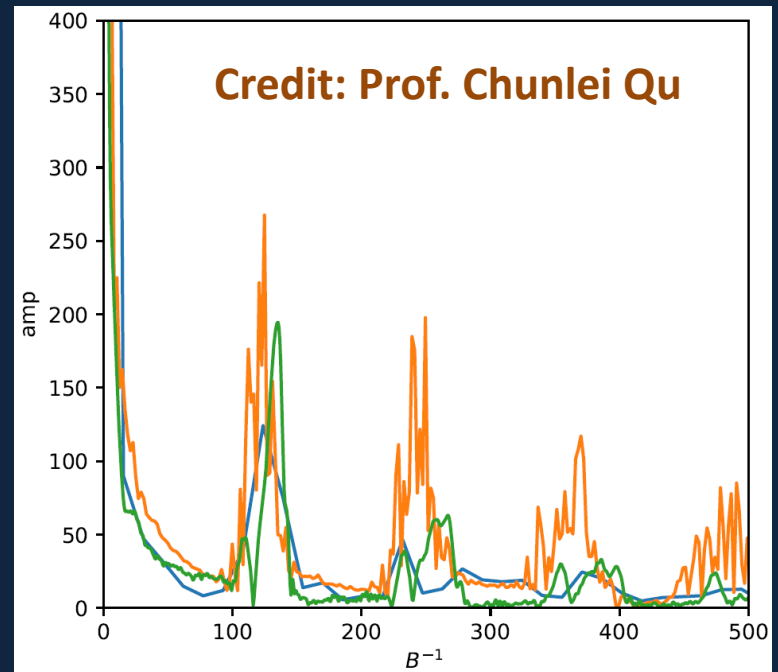


After baseline subtraction: peak spacing
 ~ 0.82 mT.

Aharonov-Bohm (AB) Oscillations

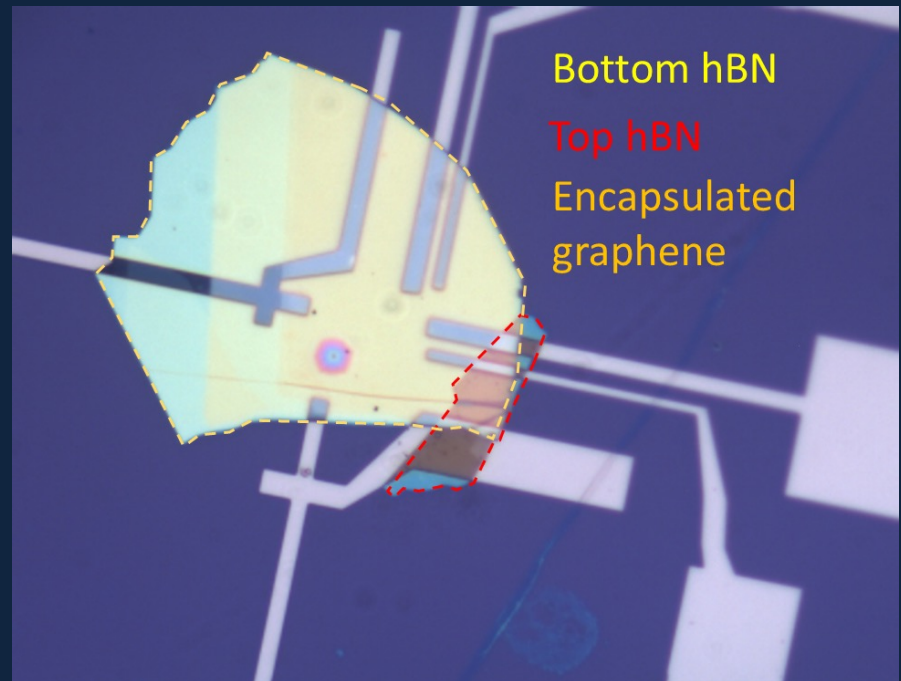
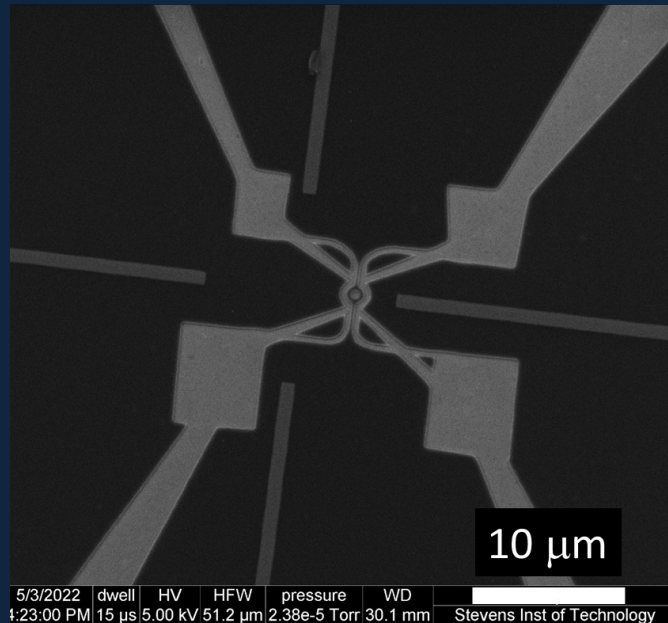
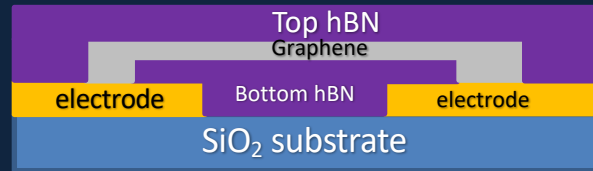


h/e oscillation frequencies corresponding to the different ring radii



Calculations not included defects, edge states, spin-orbit-coupling, top and side gate potentials, temperature effects, etc.

Enhanced Design, Fabrication & Gate-Tuning



Limitations

- **Sagnac effect:** a phase coherent effect where rotations of the ring result in a shift in the interference pattern proportional to the rotation rate.

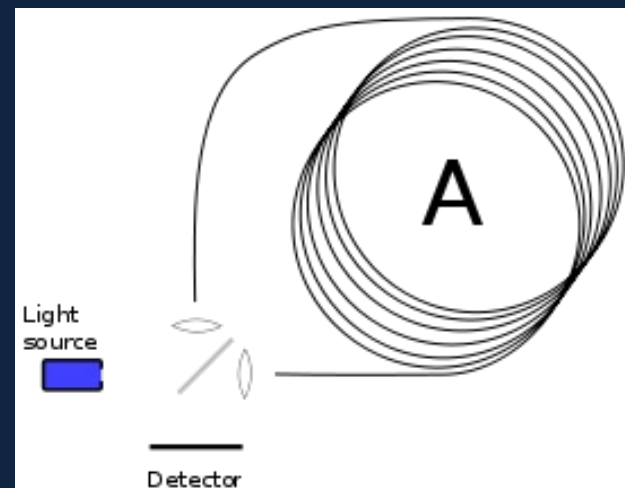
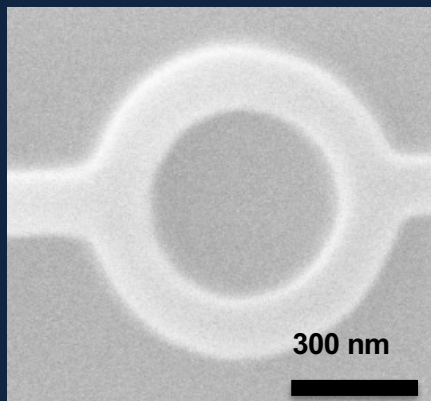
$$mc^2 / \hbar\omega \sim 10^5$$

$$\Delta\phi = 2m A \Omega / \hbar$$

$$G = I / V = (e^2 / h) \cos^2(\Delta\phi + \theta)$$

Credit: Prof. Chris Search

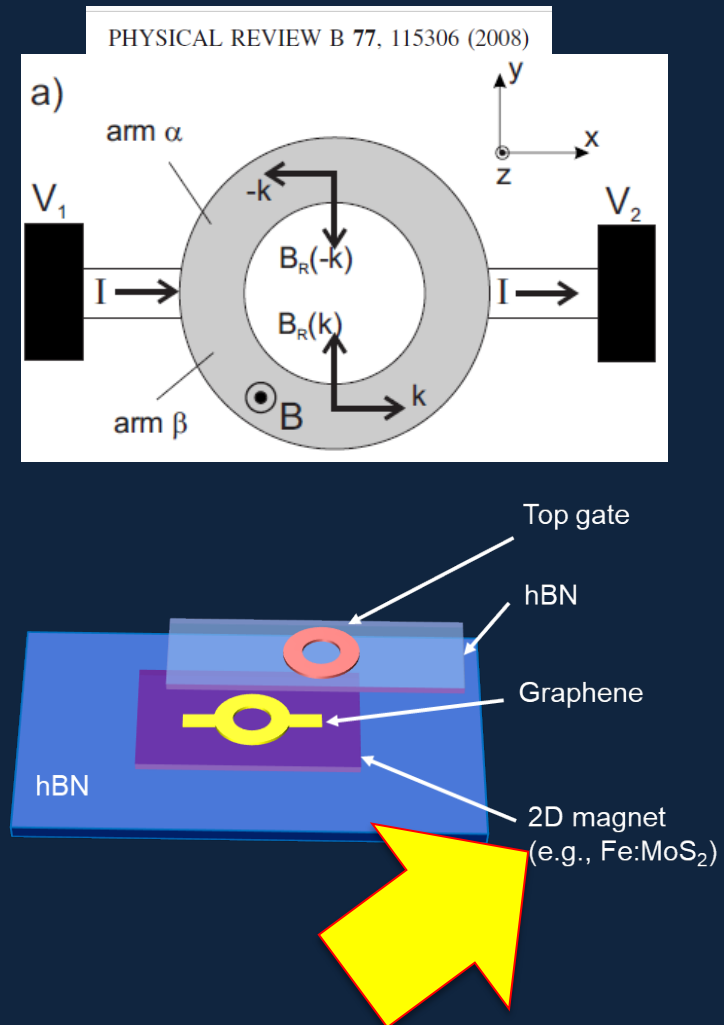
- *But, in graphene nanorings, Sagnac effect is not enough to create a measurable conductance change (limited phase coherent length).*
- The phase change must be enhanced to the detectable levels.



https://en.wikipedia.org/wiki/Sagnac_effect

Possible Solutions

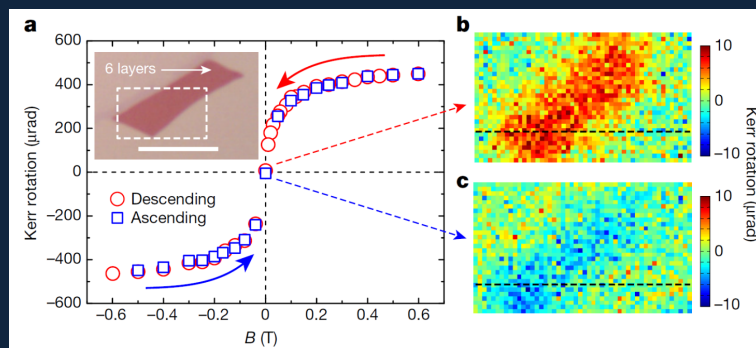
- Required Conditions:
 - A quasi-one-dimensional ring of radius r_0
 - Arms behave as a ballistic conductor
 - Ring coupled to a bias voltage V_1 - V_2
 - Perpendicular to the plane of the ring a magnetic field \mathbf{B} and electric field \mathbf{E} are applied
- Consider the following effects:
 - Zeeman splitting (due to the applied magnetic field)
 - Rashba spin-orbit interaction (due to the applied electric field and the geometry of the ring)



2D Ferromagnetic Crystals

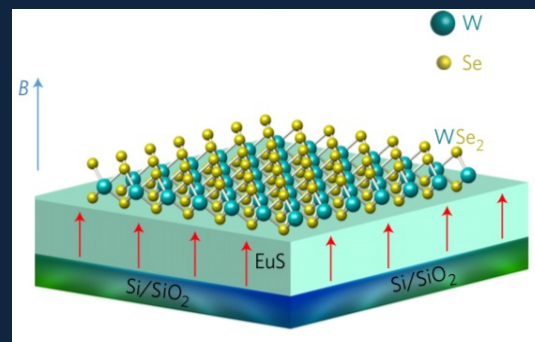
- In early 2017, the first observations of ferromagnetism at **cryogenic temps** were reported.
- CrI₃ on EuS, WSe₂ monolayers on EuS, WSe₂ monolayers on 10 nm CrI₃.

exfoliated, insulator or conductor, unstable in air



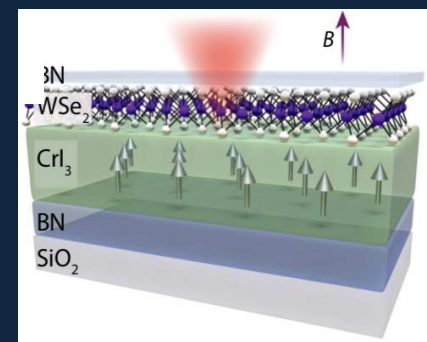
CrI₃ on EuS → $T_c \sim 45\text{K}$

Gong, et al., *Nature* **546**, 265 (2017)



WSe₂ on EuS → $T_c \sim 16.5\text{K}$

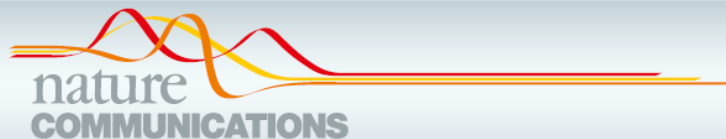
Zhao et al., *Nat. Nano.*, **12**, 757 (2017)



WSe₂/CrI₃ → $T_c \sim 61\text{K}$

Zhong et al., *Sci. Adv.*, **3**, 6586 (2017)

CVD-grown Fe:MoS₂ Monolayers

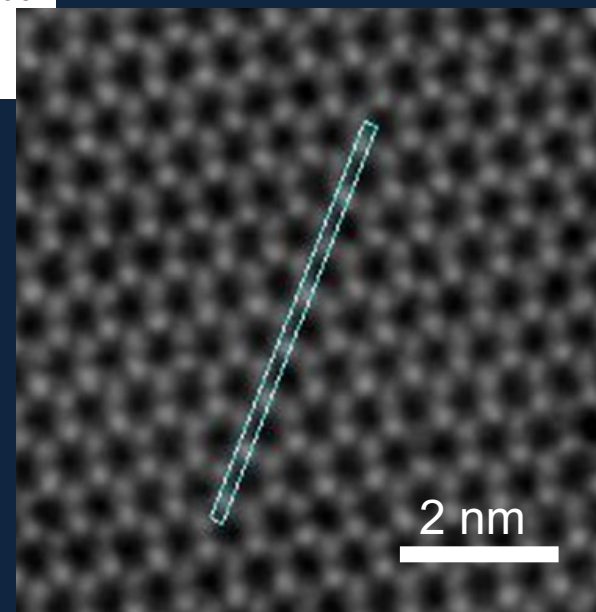
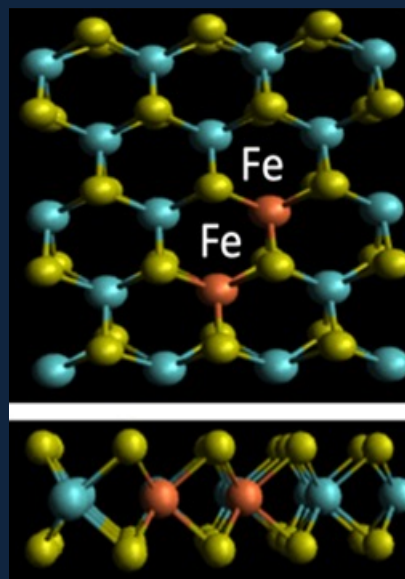
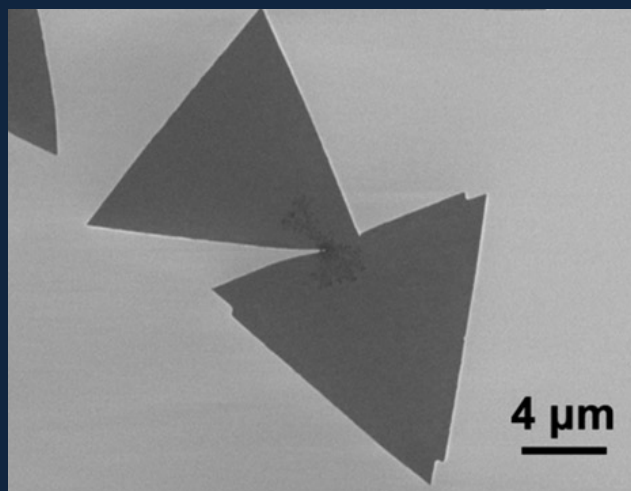
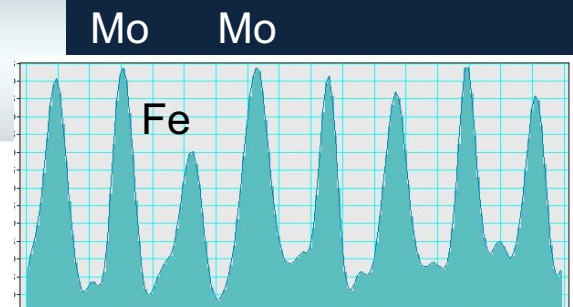


ARTICLE

<https://doi.org/10.1038/s41467-020-15877-7>

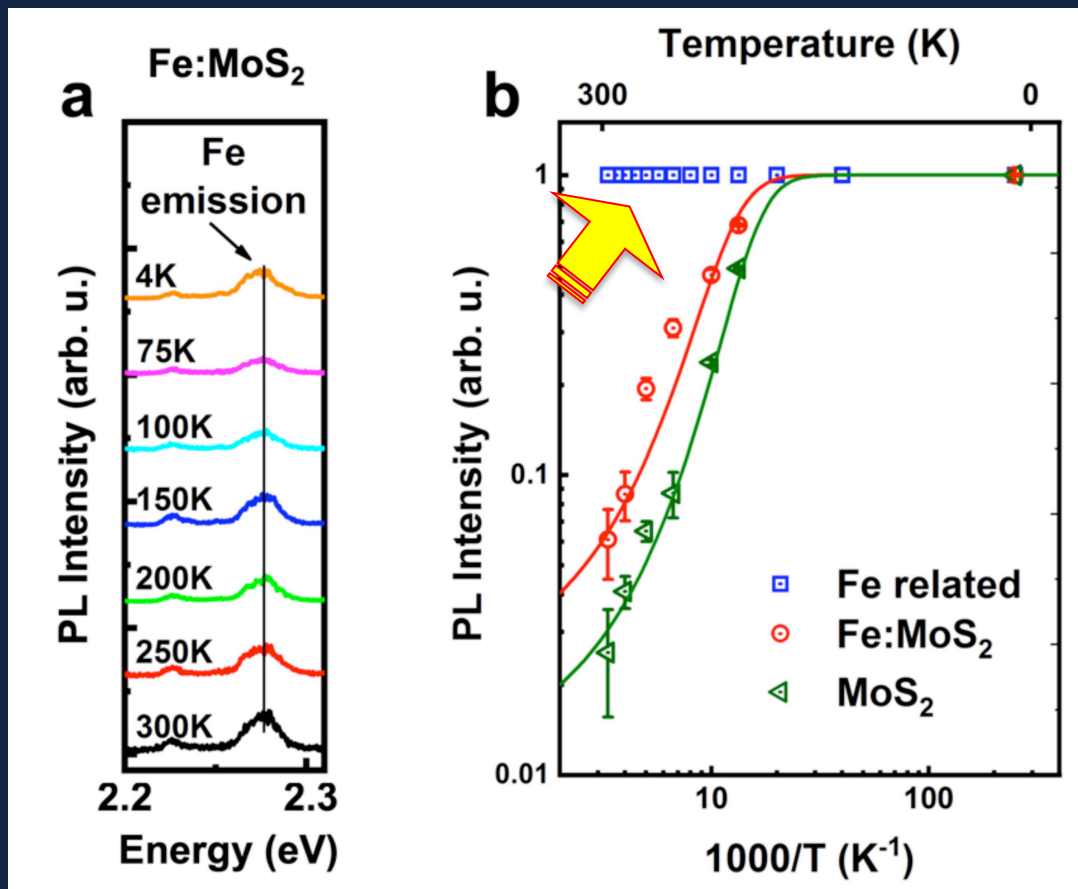
OPEN

Enabling room temperature ferromagnetism in monolayer MoS₂ via in situ iron-doping



Terrones group (Penn State)

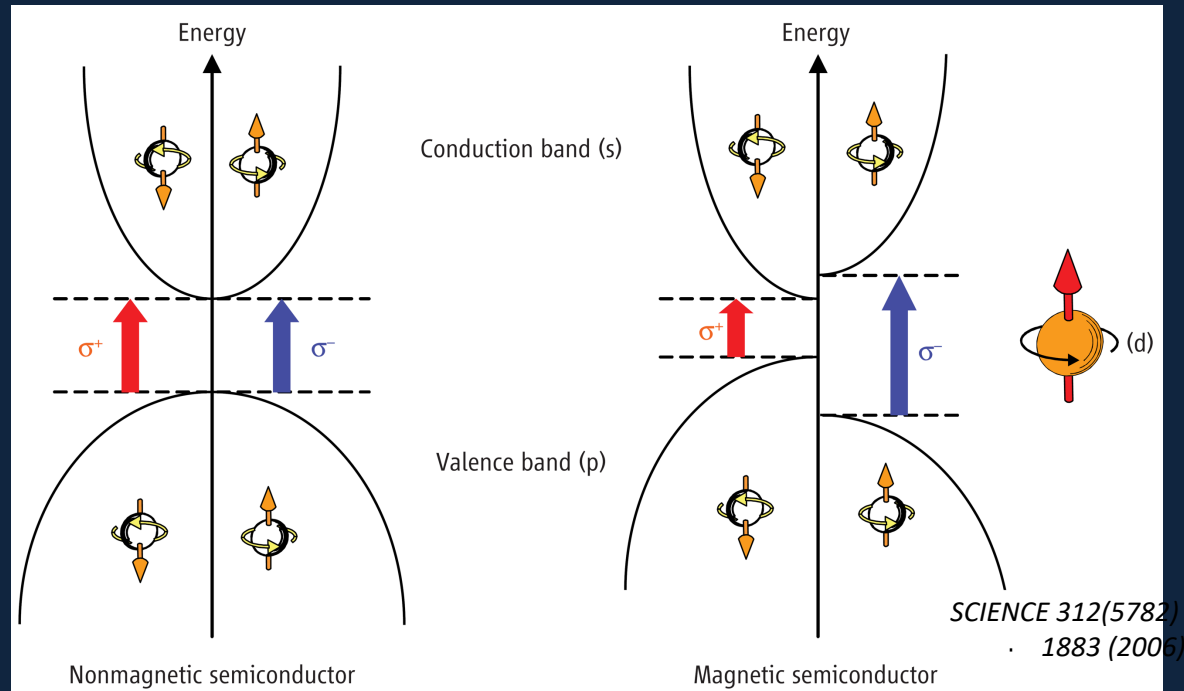
Fe-related PL Emission



Measured at Strauf Lab (Stevens)

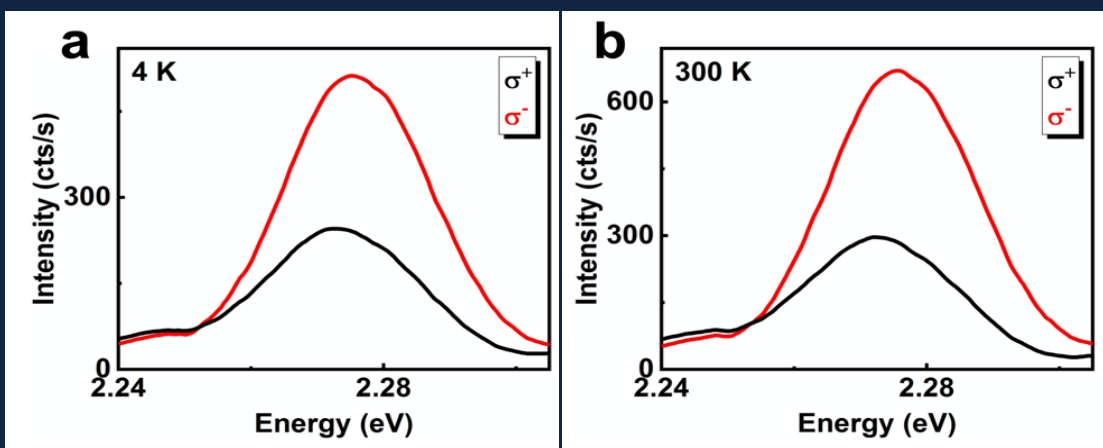
- Integrated PL for the bandgap emission in MoS₂ (green triangle), Fe:MoS₂ (red circle) and for the Fe-related emission (blue square).
- Solid red and green lines - standard Arrhenius fits for the exciton emission

Zeeman Splitting and Magnetic Circular Dichroism (MCD) Effects

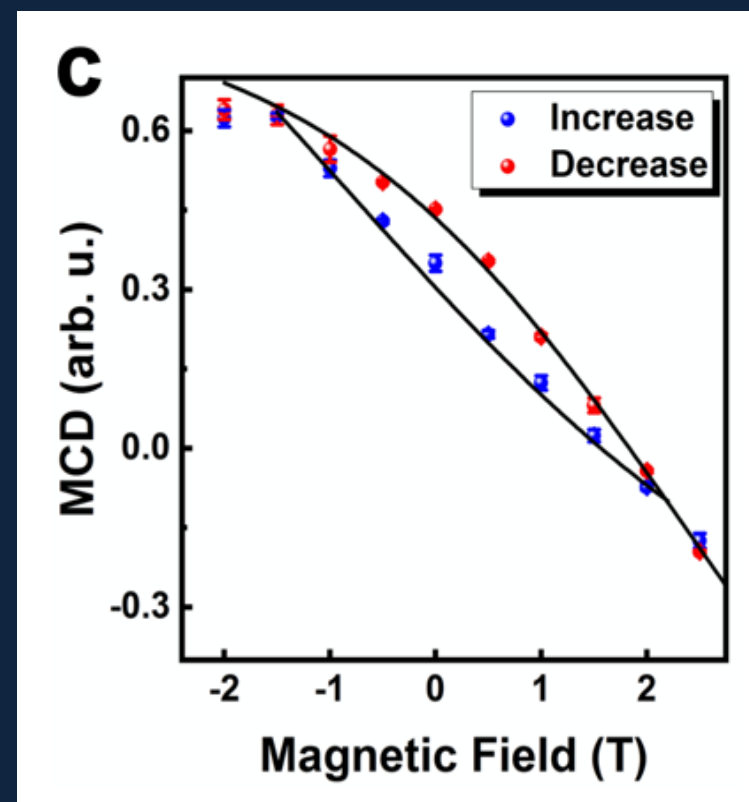


- (Left) Nonmagnetic semiconductors
- (Right) In magnetic semiconductors: the conduction band and valence band are split depending on the spin direction (**Zeeman splitting**).
- This spin-polarized semiconductor band structure alters the absorption of clockwise and counterclockwise-polarized light (**MCD effect**).

Magneto-PL (Fe-related)



- The transition metals' luminescence loses its CD above T_C
 - CD at 300K - Fe:MoS₂ is ferromagnetic at RT
- Light absorption - related to the Zeeman shifts
 - Hysteresis loop - ferromagnetic nature of emission.

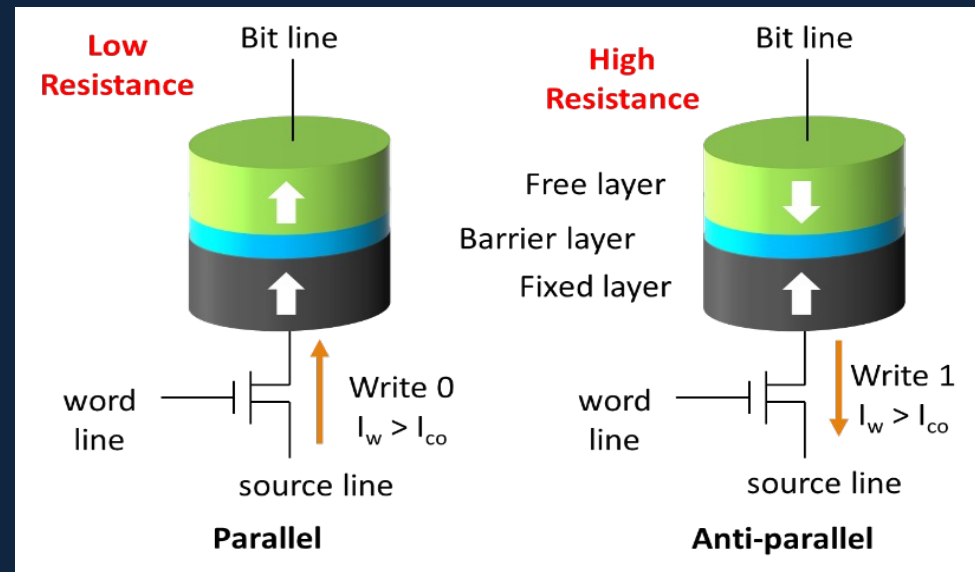


Measured at Strauf Lab (Stevens)

Magnetic Tunnel Junction (MTJ)

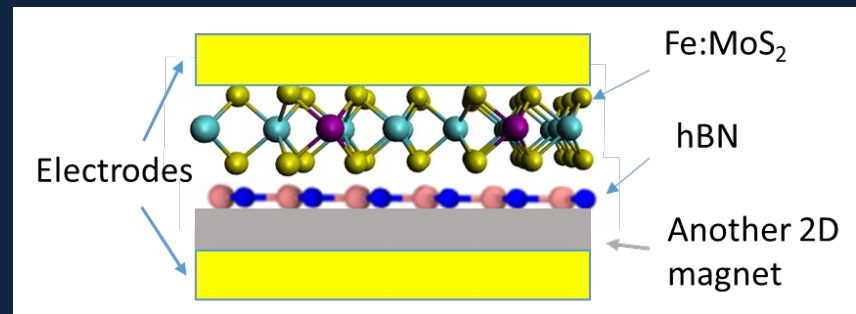
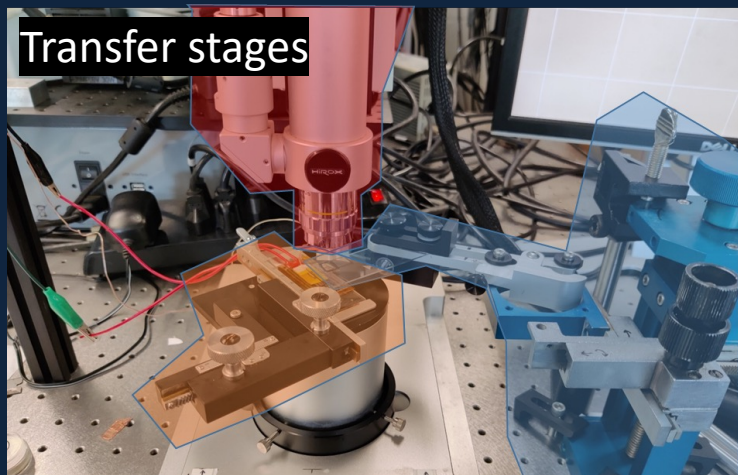
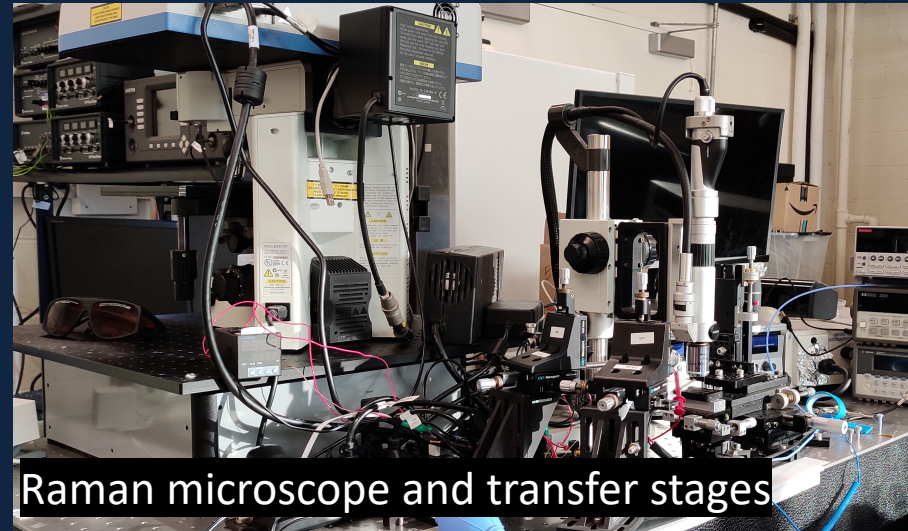
- Electrons flow through the MTJ to transfer spin angular momentum between the magnetic layers.

→ Changing the magnetic state of the free layer, and thus writing information.

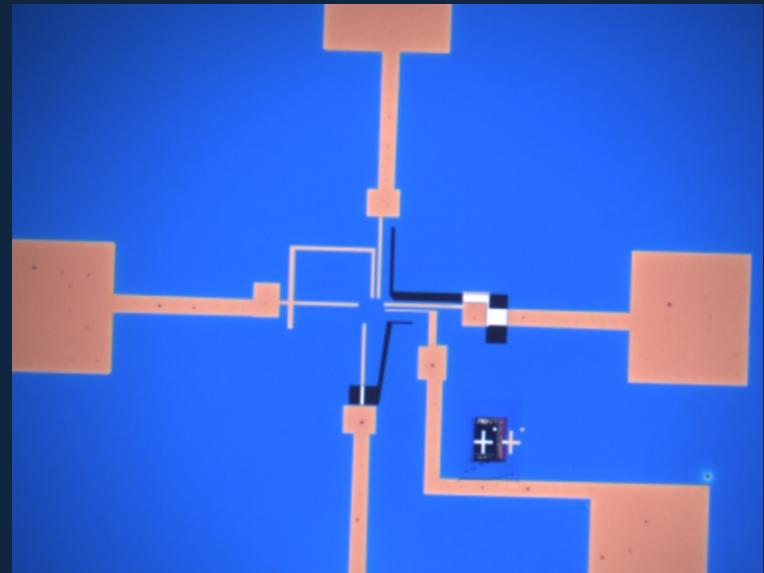
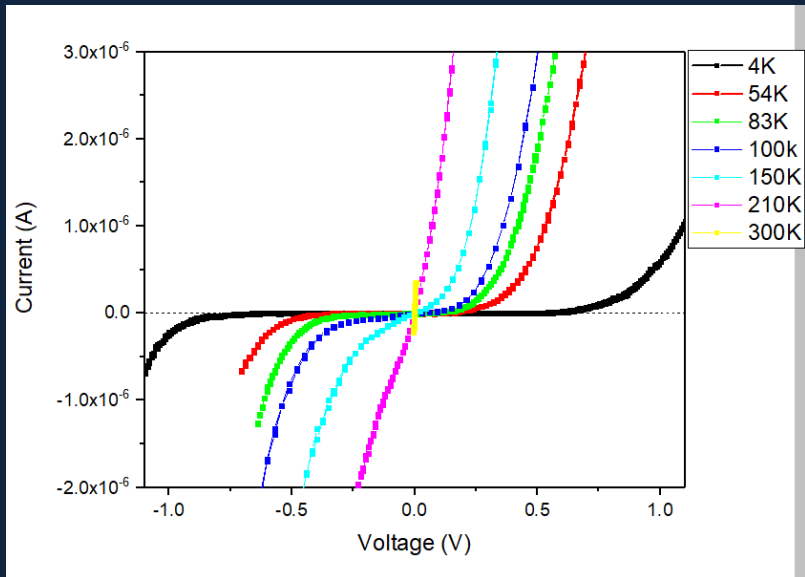


The **free layer** stores information, and the **fixed layer** provides a reference frame required for reading and writing.

Magnetic Tunnel Junction in 2D

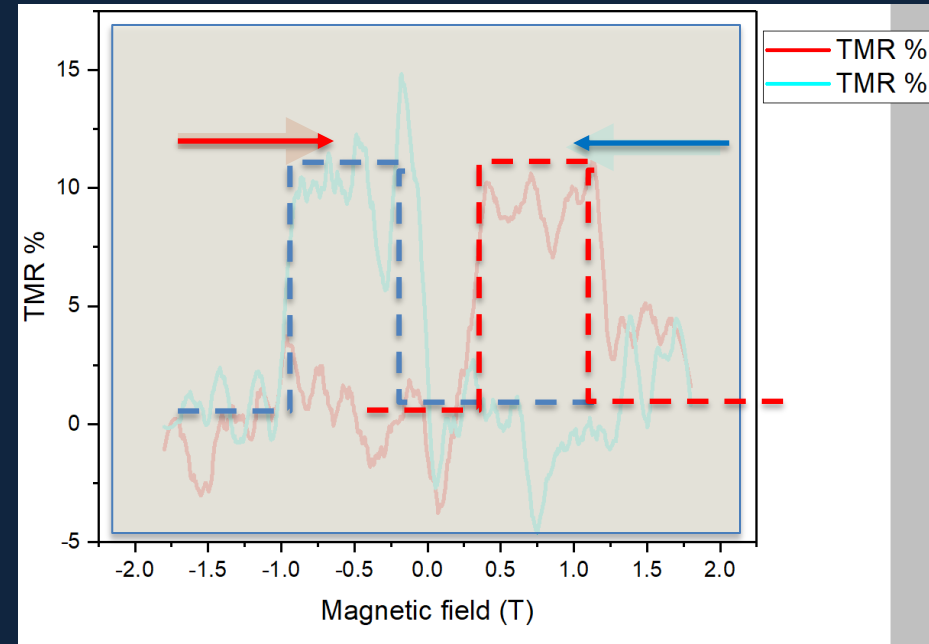
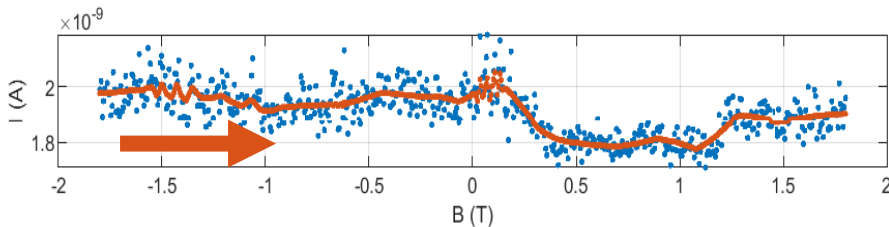
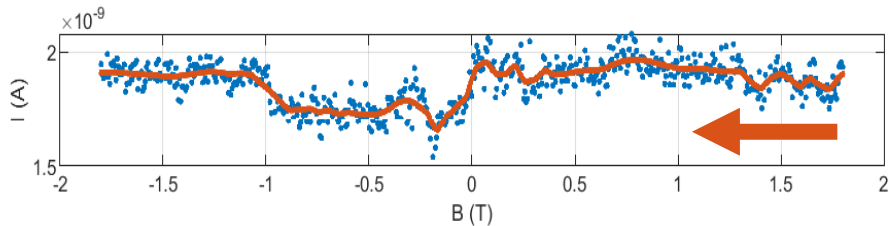


Tunneling Characteristics of Fe:MoS₂-based MTJ



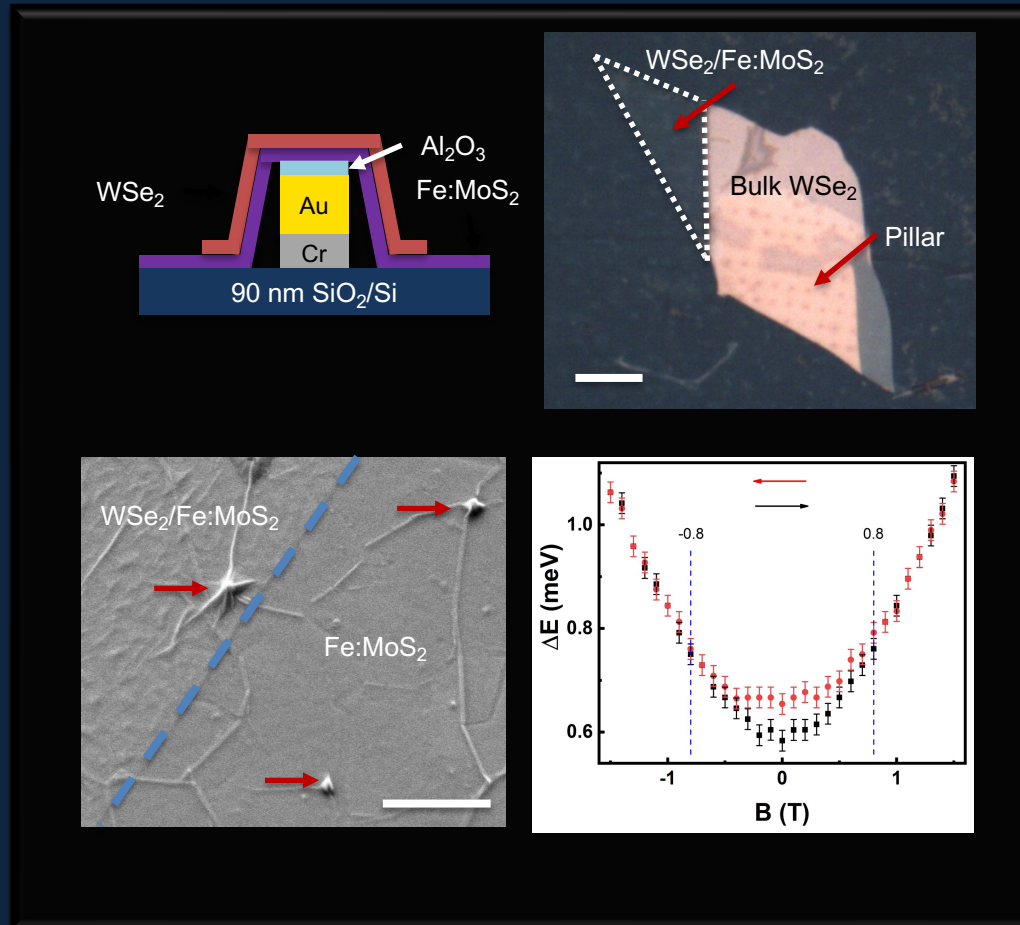
Tunneling through 2D layers - below 150K charge carriers in semiconductor start freezing; the resistance increases.

Change of Magnetic States



Demonstrating the control of
magnetoresistance

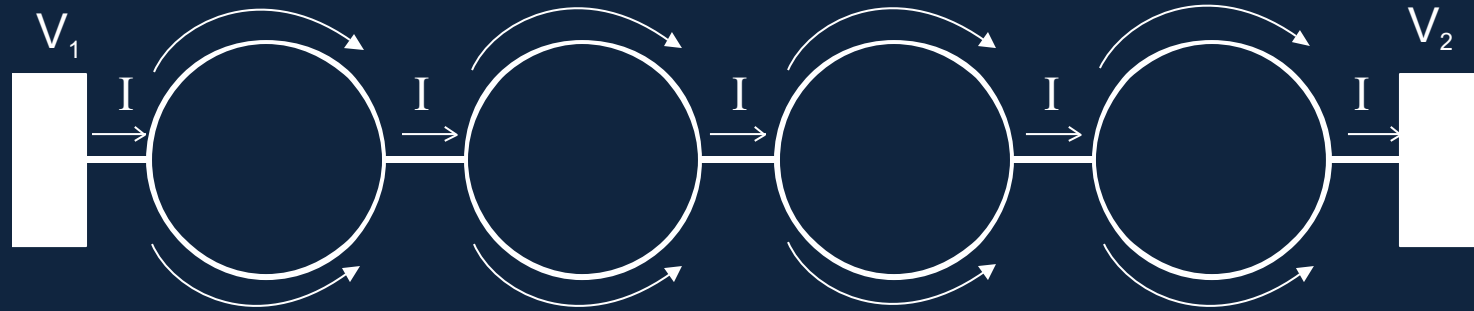
Magnetic Proximity Coupling



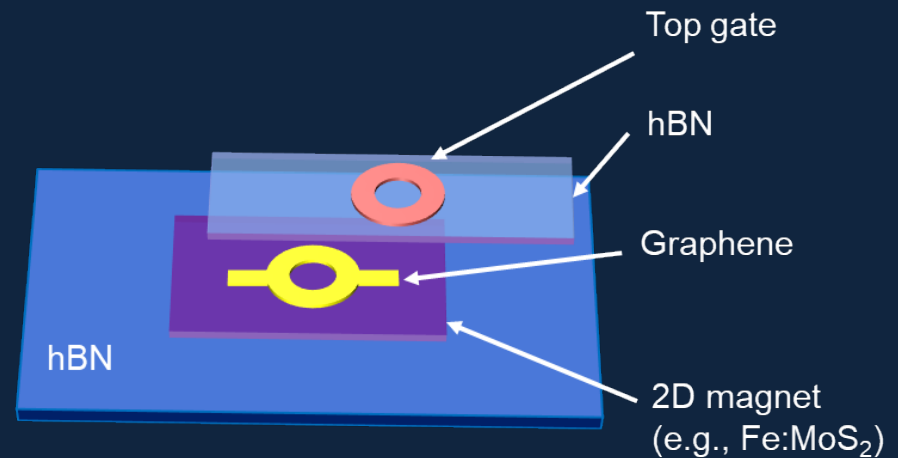
Strauf and Yang

unpublished

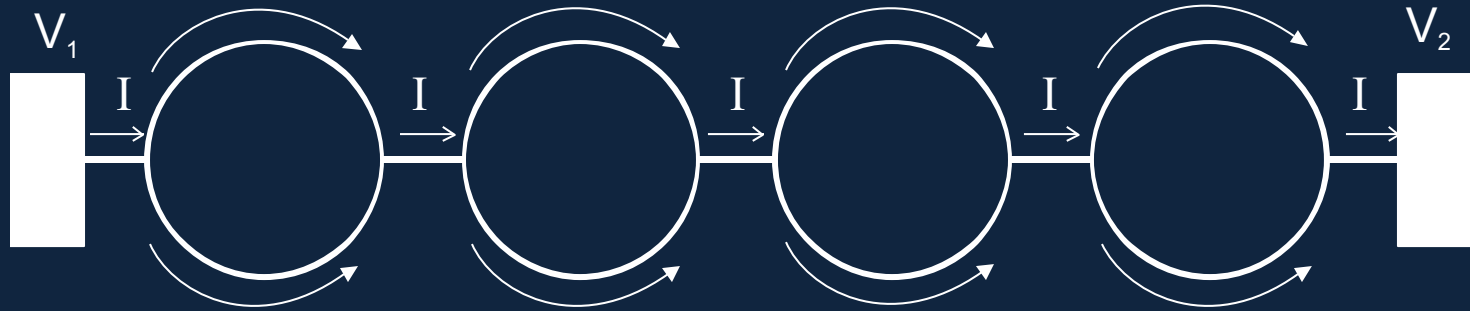
Enhancing Phase Change



- The phase change may be enhanced by incorporating **2D magnets** and **the gate-potential control** → Realizing on-chip electron interferometers.



Linear Array of Graphene Rings



$$G^{-1} \propto N \left(\Delta \Phi_s / 2 \right)^2$$

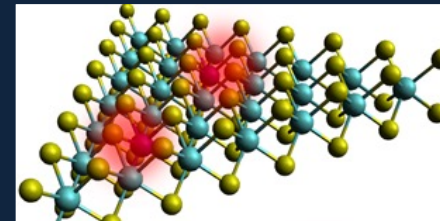
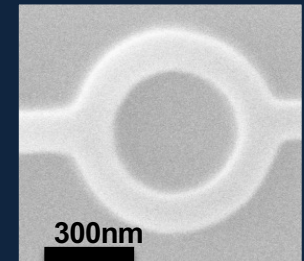
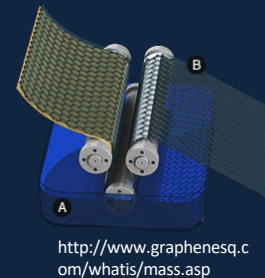
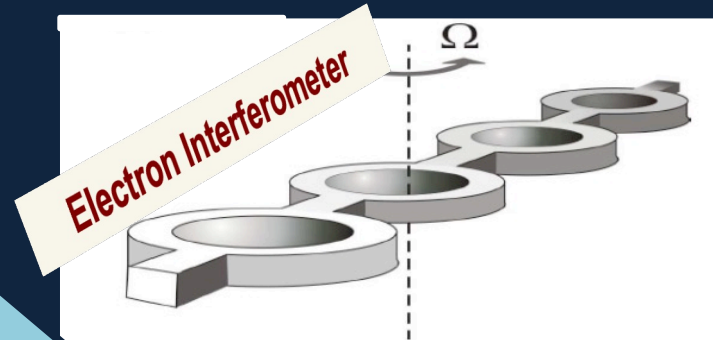
Sagnac phase shift is independent of the center of rotation

- If we fabricate 3×10^6 rings ($1 \mu\text{m}$ ring radius), *assuming there is complete dephasing of electrons in the branches between adjacent rings*, this could yield an effective phase shift 0.1 radians at 1 Hz of rotation (further verification is required).

Existing Inertial Rate Sensing Technologies



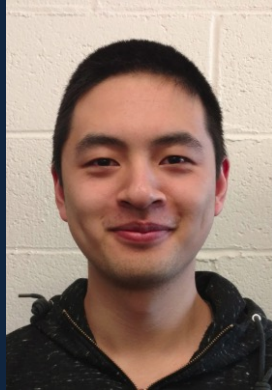
Future: High-g Survivable, Chip-Scale Technologies



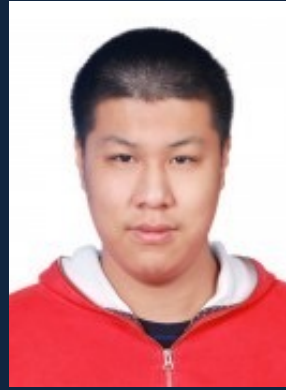
Acknowledgements



Abdus Sarkar



Siwei Chen



Zitao Tang



Mengqi Fang



Shichen Fu



Kyungnam Kang



Stefan Strauf



Chunlei Qu



Aron Cummings



Greg Hader



Yuping Huang



THANK YOU

| Stay connected with us online.

